HHS Public Access

Author manuscript

Anal Biochem. Author manuscript; available in PMC 2019 December 31.

Published in final edited form as:

Anal Biochem. 1999 April 10; 269(1): 162–167. doi:10.1006/abio.1999.4011.

Lifetime-Based pH Sensors: Indicators for Acidic Environments

Hai-Jui Lin, **Henryk Szmacinski**, **Joseph R. Lakowicz**[1]

Center for Fluorescence Spectroscopy, Department of Biochemistry and Molecular Biology, University of Maryland School of Medicine, 725 West Lombard Street, Baltimore, Maryland 21201

Abstract

We characterized the pH-dependent intensity decays of three fluorophores, Oregon green 514 carboxylic acid, Cl-NERF, and DM-NERF, using frequency-domain fluorometry, with the objective of identifying lifetime-based sensors for low pH values. These three probes were originally designed as dual excitation wavelength–ratiometric probes, with high photostability and high quantum yields in aqueous solutions. We found that their fluorescence intensity decays were strongly dependent on pH. Moreover, global intensity decays analysis reveals that these probes have double exponential intensity decays at intermediate pH values and that the decay time amplitudes are greatly dependent on pH. The longer lifetime components originated from the unprotonated forms and the shorter components from the protonated forms. Both forms can emit fluorescence at intermediate pH values. The apparent pK_a values were also determined from the titration curves of phase angles and modulations versus pH for the purpose of pH sensing. The apparent pK_a values range from pH 3 to 5, a range where lifetime-based sensors are not presently reported. Since these probes show low pK_a values and display substantial phase and modulation changes with pH, they are suitable as lifetime-based pH sensors to monitor the pH changes in acidic environments. One potential application of these probes is to trace the pH in different cellular compartments.

Fluorescence sensing techniques are advancing very rapidly and have been widely used for quantitative measurements in clinical chemistry and cell biology. Fluorescence detection can provide high sensitivity, and suitably designed fluorophores provide the ability to monitor living cells with high analyte selectivity. For example, fluorescence wavelength ratiometric sensing has been widely used to follow the biochemical and ionic changes in cells (1). Furthermore, with the help of confocal microscopy, fluorescence lifetime imaging (2, 3), and two-photon excitation techniques (4), imaging of pH, calcium, or proteins (5) in organelles and cellular compartments can be accomplished. In recent years a number of new pH probes have been synthesized and utilized for pH sensing based on fluorescence emission ratios (6–8), excitation ratios (6, 7, 9, 10), and fluorescence lifetimes (11–13).

Cellular pH measurements based on fluorescence have also been widely utilized. As examples, fluorescence has been used to measure the cytosolic pH gradient in developing zygotes (14, 15), to trace the endosomal pH evolution along the endocytosis pathway (16, 17), and to determine the phagosomal pH of microphages (18). In recent years, we have seen

[1]To whom correspondence should be addressed.

the introduction of fluorescence lifetime-based techniques for cellular fluorescence imaging. Fluorescence lifetime-based sensing can be accomplished by several approaches, such as time-resolved measurements (19, 20), time-gated techniques (21, 22), and frequency domain measurements (23–26). These methods allow localized quantities and imaging of chemical species in cells.

In the present report, we describe the spectrometric characteristics of three lifetime-based pH sensors, Oregon green 514 carboxylic acid, Cl-NERF, and DM-NERF. These probes were first introduced by Molecular Probes (Eugene, OR) and used as excitation ratio probes for the pH determinations in acidic environments (27, 28). Both their protonated and unprotonated forms have high extinction coefficients between 470 and 520 nm and emit bright yellowish light. The absorption spectra of the protonated species are blue-shifted relative to the unprotonated forms. They are considered better pH sensors than fluorescein because of their greater photostability and the possibility of wavelength-ratiometric measurements. We found that both forms (protonated and unprotonated) display emission with distinct intensity decays that result in significant pH-dependent phase angles and modulations. Using their appropriate conjugates, these probes could be introduced into the cells and trace the pH distribution in acidic cellular compartments.

MATERIALS AND METHODS

The pH probes, Oregon green carboxylic acid 514, DM-NERF, and Cl-NERF, were purchased from Molecular Probes (Eugene, OR) and used without further purification. Their chemical structures are shown in Fig. 1. The other chemicals used for preparing different pH buffer solutions were obtained from Sigma (St. Louis, MO) and Aldrich (Milwaukee, WI). The buffer series included 50 mM of citrate buffer, phosphate buffer, Tris buffer, and carbonate buffer, covering the pH range from 2 to 9. All these buffers contained 100 mM of KCl to maintain a constant ionic strength. Aqueous stock solutions of each probe were added to the buffer solutions to prepare the samples of final concentration of 1.5 μM for all the spectrophotometric measurements.

Absorption spectra were performed with a Hewlett–Packard 8453 Spectrophotometer. Fluorescence emission spectra were measured using an Aminco Bowman Series AB2 Luminescence Spectrometer with excitation wavelengths of 488 and 514 nm. The time-resolved fluorescence intensity decays were measured using frequency-domain phase/modulation instrumentation (ISS, Inc.). The excitation source for the frequency-domain measurements was an air-cooled argon ion laser (543-AP Omnichrome), with its 488-nm output amplitude modulated by an electrooptic modulator (ISS, Inc.). A mode-locked argon ion laser with output at 514 nm was also used for the phase and modulation acquisition at a single frequency of 75.47 MHz. An aqueous solution of erythrosin B (BDH, UK) with a fluorescence lifetime of 80 ps was used as the lifetime reference. In order to cut off the scattered excitation light, long pass filters from Corning (above 510 and 540 nm) were placed on the emission side of the sample.

The fluorescence intensity decays were recovered from the multifrequency data and analyzed with single or double exponential decay models,

$$I_{\mathrm{k}}(t) = \sum_{i=1,k}^{2} \alpha_{ik} e^{-t/\tau_i} \quad (1)$$

where $I_k(t)$ is the fluorescence intensity decay at each pH (k) value, and α_{ik} is the amplitude for individual lifetime $\tau_i(\Sigma\alpha_{ik} = 1)$. The fractional intensity f_{ik} of each decay component ($f_{ik} = \alpha_{ik}\tau_i/\Sigma\alpha_{ik}\tau_i$) was also determined. Detailed descriptions of the theories and instruments have been published previously (29, 30). For global intensity decays analysis, the individual lifetime τ_i was set as the global parameter, but the amplitudes α_{ik} were dependent on the pH environments.

RESULTS

Oregon green 514 carboxylic acid (OG514)[2] is a pentaflouorofluorescein derivative with its absorption maximum red-shifted about 25 nm relative to that of fluorescein. DM-NERF and Cl-NERF are derived from dimethyl and chloro substitution on Rhodol Green carboxylic acid and can be considered as structural hybrids of fluorescein and rhodamine (Fig. 1). All these probes are claimed to have greater photostability than fluorescein (Molecular Probes' Handbook of Fluorescence Probes and Research Chemicals, 6th ed., p. 563). Absorption and emission spectra of the three probes at different pH values are shown in Fig. 2. Protonation of these probes resulted in decreased extinction coefficients and quantum yields, as well as the blue shift of their absorption spectra. The pH-dependent shifts of the absorption spectra indicate these probes are suitable for excitation wavelength ratiometric measurements. The emission maxima of these probes are shown to be pH-insensitive by comparing the normalized spectra of these probes at high and low pH values. However, the emission intensities increase dramatically with increasing of pH due to the higher quantum yields of the protonated forms than those of the unprotonated forms (Table 1). In Fig. 3, we show the excitation intensity ratios of the three probes at various pH values. The pK_a values observed by fluorescence measurements are quiet close to the ground state pK_a values listed in Table 1, which suggests that pK_a changes and excited state reactions do not substantially affect the spectrum of these probes. Similar results for these probes at different excitation wavelengths have been reported (1, 16, 27). The intensity ratios are dependent on the excitation wavelengths and instrumentation we used.

The shift of the absorption spectra and the changes of emission intensity indicate that more than one fluorescent species exist in aqueous solution. These species are the probes at different protonation levels, showing different extinction coefficients and quantum yields. If all these forms can fluoresce, changes of the quantum yields could be attributed to the different intensity decays of these forms. If multiple species exist with different decay times, then these probes can be used for lifetime-based measurements, as well as for wavelength-ratiometric measurements. It has been reported earlier that the pH sensitive range could be significantly expanded by using wavelength-ratiometric probes with lifetime-based measurements (11).

[2]Abbreviation used: OG514, Oregon Green 514 carboxylic acid.

To characterize these probes as lifetime-based sensors, we measure their frequency domain intensity decays (Fig. 4). The frequency responses of all these probes display a significant shift to high-modulation frequencies in low pH environments, indicating a shorted mean lifetime at low pH. The intensity decays of each probe were satisfactorily fitted to the two-exponential model for a wide range of pH values, except for very low values. Global analysis was performed by assuming that two fluorescent species exist in aqueous solution and that each form displays the single exponential decays τ_1 (acid form) and τ_2 (basic form). The two lifetimes were taken as global parameters, which are independent of pH. In the fitting process, the values of the preexponential factors (α_1 and α_2) were variable, reflecting the relative amount of each form at each pH value. The results of intensity decay analysis are summarized in Table 2, including the fractional intensity f_i of each decay component ($f_i = \alpha_i\tau_i/\Sigma\ \alpha_i\tau_i$). Intensity decays at extremely low pH values of 0.9 were also measured. The analysis results revealed another decay time of 1.55 ns for OG514, 1.22 ns for Cl-NERF, and 2.18 ns for DM-NERF. Nevertheless, there was only a minor change in the absorption and emission spectrum below pH 2.0. This additional component at low pH may be due to a second protonated form of these probes, which can fluoresce and is present only at very low pH. All three probes displayed significant changes in lifetime as the pH varied from 3 to 6. The largest change in lifetime was observed for Cl-NERF ($\tau_2/\tau_1 = 2.74$). Significant changes were also found for OG514 ($\tau_2/\tau_1 = 1.78$) and DM-NERF ($\tau_2/\tau_1 = 1.63$).

The high pH sensitivity of the intensity decays of these probes results in significant changes of the phase angle and modulation, especially at modulation frequencies ranging from 40 to 100 MHz (Fig. 4). The modulation frequency of 75.47 MHz was chosen to describe the pH-dependent phase angle and modulation changes (Fig. 5). This frequency of 75.47 MHz is the fundamental frequency of the mode-locked Ar-ion laser and close to that of many mode-locked lasers. In Table 1, we summarized the apparent pK_a values and the magnitude of the changes in phase angle and modulation at the excitation wavelengths of 488 and 514 nm (Ar-ion laser). Since OG514 is a polyfluorinated fluorescein-based dye, its pK_a values should be much lower than those determined for fluorescein because of the presence of electron-withdrawing fluorine. Similarly, the amine substituents of DM-NERF and Cl-NERF reduce their pK_a values, the presence of methyl groups on DM-NERF increases the values to around five, and the presence of chloro groups on Cl-NERF reduces the values to around three. While it is clear that the probes display pH-dependent ionization, we can not assign with certainty the pK_a values with ionizable groups on the probes. Consistent with the lifetime changes, Cl-NERF displayed the largest changes in phase angle (27°) and modulation (0.36) from its protonated form to unprotonated form, and DM-NERF displayed the smallest changes (Table 1). These pH-dependent phase and modulation data were fitted to the Henderson–Hasellboch equation to determine the apparent pK_a values. Cl-NERF displays the lowest apparent pK_a value, and DM-NERF displays the highest value. Since the useful pH sensing range will be pK_a ± 1, the pH probes discussed here provide a working range from pH 2 to 6. Moreover, the apparent pK_a values from phase angle and modulation are dependent on the excitation wavelength. The main reason for the increase of pK_a at 488 nm excitation is due to the greater contribution of the protonated form to the mean fluorescence lifetime (presenting as the lower phase angle and higher modulation) at the

shorter excitation wavelength. Higher apparent pK_a values are expected if the excitation wavelength will be shorter than 488 nm.

DISCUSSION

The increasing availability of lifetime sensing instruments and lifetime imaging microscopes requires a selection of lifetime sensors. New fluorophores with desirable selectivity to different cellular components have been introduced into living systems as indicators to study different intracellular species. It has already been reported that some ratiometric probes display not only changes of their intensity ratios, but also useful changes in their fluorescence intensity decays (11). Several pH-sensitive probes like carboxy-SNAFL-1, BCECF, and DM-NERF have been used in time-resolved fluorescence microscopy to determine the cytosolic pH (21, 22).

All three probes discussed here display significant phase angle and modulation sensitivity to pH, especially in acidic pH regions close to their pK_a values. Table 1 shows that apparent pK_a can be shifted to lower values by changing the excitation wavelength from 488 to 514 nm, which provides a possibility to extend the pH working range of these probes. While not studied here, it is likely that the apparent pK_a values can also be modified by selection of the emission wavelength. The other fluorescence characteristics, such as high quantum yields, good photostability, and being excitable by the major emitting lines of Ar-ion laser, support these probes as promising pH indicators for fluorescence lifetime microscopy. Because their responses are more sensitive to the low pH environment than to the near-neutral cytosol, these probes may be used to trace the pH evolution in acidic cellular compartments. These compartments can be vacuoles of yeast (31), endosomes (4), and phagosomes (18) of macrophages and endocytic systems in different cell lines (16, 32, 33) or in microorganisms (17). Similar to the strategies used for pH sensing with fluorescein (16, 34), these lifetime sensors can be linked to different macromolecules such as dextran, zymosans, and soluble exogenous antigens. Then these conjugates can be introduced into different cellular compartments through endocytosis, fluid-phase pinocytosis, or phagocytosis. After that they will be processed and transported to different destinations via diverse pathways. If these conjugates do not degrade and keep all their spectrometric properties, they can reflect the pH differences within the cellular compartments.

REFERENCES

1. Dunn KW, Mayor S, Myers JN, and Maxfield FR (1994) FASEB 8, 573–582.
2. Gadella TWJ Jr., Jovin TM, and Clegg RM (1993) Biophys. Chem 48, 221–239.
3. Dong CY, So PTC, French T, and Gratton E (1995) Biophys. J 69, 2234–2242. [PubMed: 8599631]
4. French T, So PTC, Weaver DJJ, Coelho-Sampaio T, Gratton E, Voss EWJ, and Carrero J (1997) J. Microsc 185, 339–353. [PubMed: 9134740]
5. Harootunian AT, Adams SR, Wen W, Meinkoth JL, Tayor SS, and Tsien RY (1993) Mol. Biol 4, 993–1002.
6. Zhou Y, Marcus EM, Haugland RP, and Opas M (1995) J. Cell. Physiol 164, 9–16. [PubMed: 7790401]
7. Whitetaker JE, Haugland RP, and Prendergast FG (1991) Anal. Biochem 194, 330–344. [PubMed: 1862936]
8. Kurtz I, and Balaban RS (1985) Biophys. J 48, 499–508. [PubMed: 4041540]

9. Nedergarrd M, Desai S, and Pulsinelli W (1990) Anal. Biochem 187, 109–114. [PubMed: 2372106]
10. Martinez-Zaguilan R, Tompkins LS, and Lynch RM (1994) SPIE 2137, 17–28.
11. Szmacinski H, and Lakowicz JR (1993) Anal. Chem 65, 1668–1674. [PubMed: 8368522]
12. Thompson RB, and Lakowicz JR (1993) Anal. Chem 65, 853–856. [PubMed: 31831912]
13. Draxler S, and Lippitsch M (1993) Sens. Actuators B 11, 421–424.
14. Gibbon BC, and Kropf DL (1994) Science 263, 1419–1421. [PubMed: 17776513]
15. Kropf DL, Henry CA, and Gibbon BC (1995) Eur. J. Cell Biol 68, 297–305. [PubMed: 8603682]
16. Lee RJ, Wang S, and Low PS (1996) Biochim. Biophys. Acta 1312, 237–242. [PubMed: 8703993]
17. Aubry L, Klein G, Martiel J-L, and Satre M (1993) J. Cell Sci 105, 861–866. [PubMed: 7691851]
18. Vergne I, Constant P, and Lanéelle G (1998) Anal. Biochem 255, 127–132. [PubMed: 9448851]
19. Herman B, Wodnicki P, Kwon S, Periasamy A, Gordon GW, Mahajan N, and Wang XF (1997) J. Fluoresc 7, 85–91.
20. Srivastava A, and Kirshnamoorthy G (1997) Anal. Biochem 249, 140–146. [PubMed: 9212865]
21. Sanders R, Gerritsen HC, Draaijer A, Houpt PM, van Veen SJF, and Levine YK (1994) SPIE 2137, 56–62.
22. Sanders R, Draaijer A, Gerritsen HC, Houpt PM, and Levine YK (1995) Anal. Biochem 227, 302–308. [PubMed: 7573951]
23. Lakowicz JR, Szmacinski H, and Johnson ML (1992) J. Fluoresc 2, 47–62. [PubMed: 24243158]
24. Lakowicz JR, Szmacinski H, Nowaczyk K, and Johnson M (1992) Proc. Natl. Acad. Sci. USA 89, 1271–1275. [PubMed: 1741380]
25. Lakowicz JR, and Szmacinski H (1993) Sens. Actuators B 11, 133–143.
26. Lakowicz JR, Szmacinski H, Nowaczyk K, Lederer WJ, Kirby MS, and Johnson M (1994) Cell Calcium 15, 7–27. [PubMed: 8149407]
27. Whitaker JE, Haugland RP, Ryan D, Dunn K, Maxfield FR, and Haugland RP (1991) Biophys. J 59, 358a.
28. Dunn K, Maxfield FR, Whitaker JE, Haugland RP, and Haugland RP (1991) Biophys. J 59, 345a.
29. Lakowicz JR, and Maliwal BP (1985) Biophys. Chem 21, 61–78. [PubMed: 3971026]
30. Lakowicz JR (1991) in Topics in Fluorescence Spectroscopy, Vol. 1, Techniques (Lakowicz JR, Ed.), pp. 293–355, Plenum, New York.
31. Pena A, Ramírez J, Rosas G, and Calahorra M (1995) J. Bacteriol 177, 1017–1022. [PubMed: 7860582]
32. Zen K, Biwersi J, Periasamy N, and Verkman AS (1992)J. Cell Biol 119, 99–110. [PubMed: 1382079]
33. van Weert AWM, Dunn KW, Geuze HJ, Maxfield FR, and Stoorvogel W (1995) J. Cell Biol 130, 821–834. [PubMed: 7642700]
34. van Deurs B, Ropke C, and Thorball N (1984) Eur. J. Cell Biol 34, 96–102. [PubMed: 6203751]

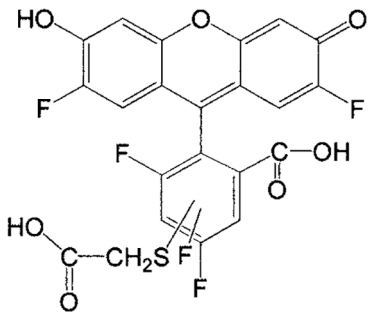

Oregon Green 514 Carboxylic Acid

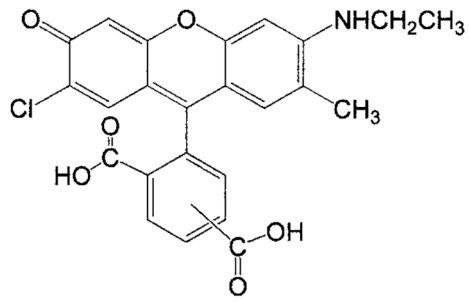

Cl-NERF

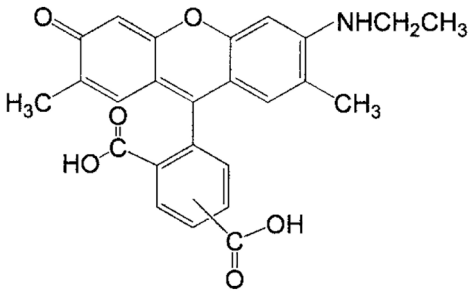

DM-NERF

FIG. 1.

Chemical structures of the three pH probes: Oregon green 514 carboxylic acid, Cl-NERF, and DM-NERF.

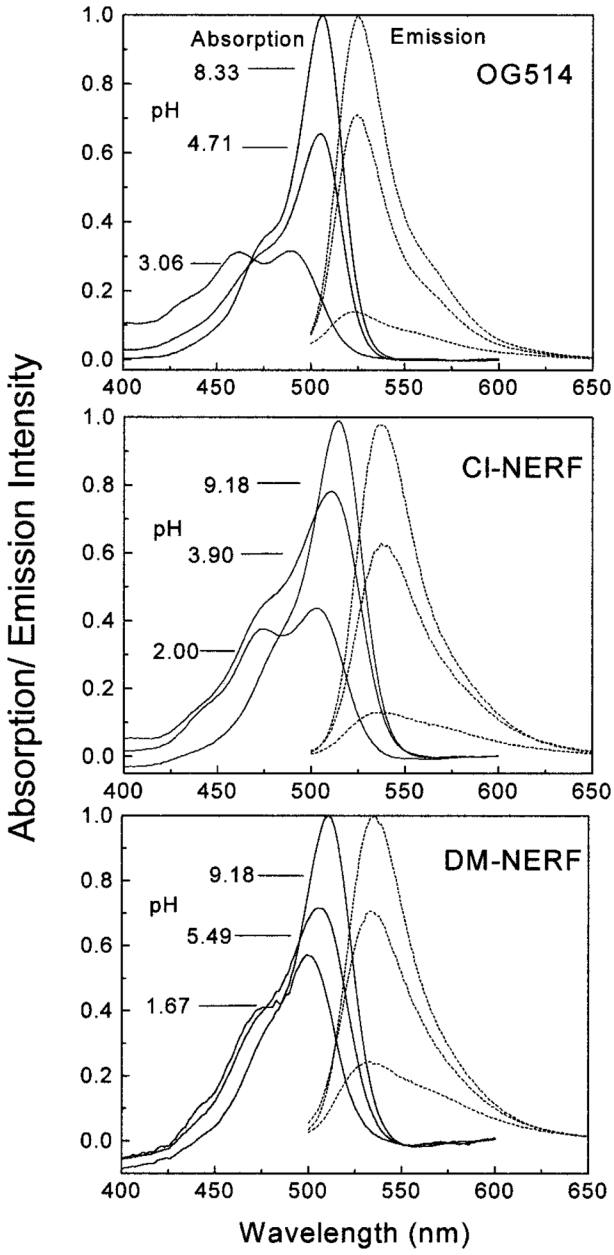

FIG. 2.

The pH-dependent absorption and emission spectra of OG514, Cl-NERF, and DM-NERF. The excitation wavelength was 488 nm.

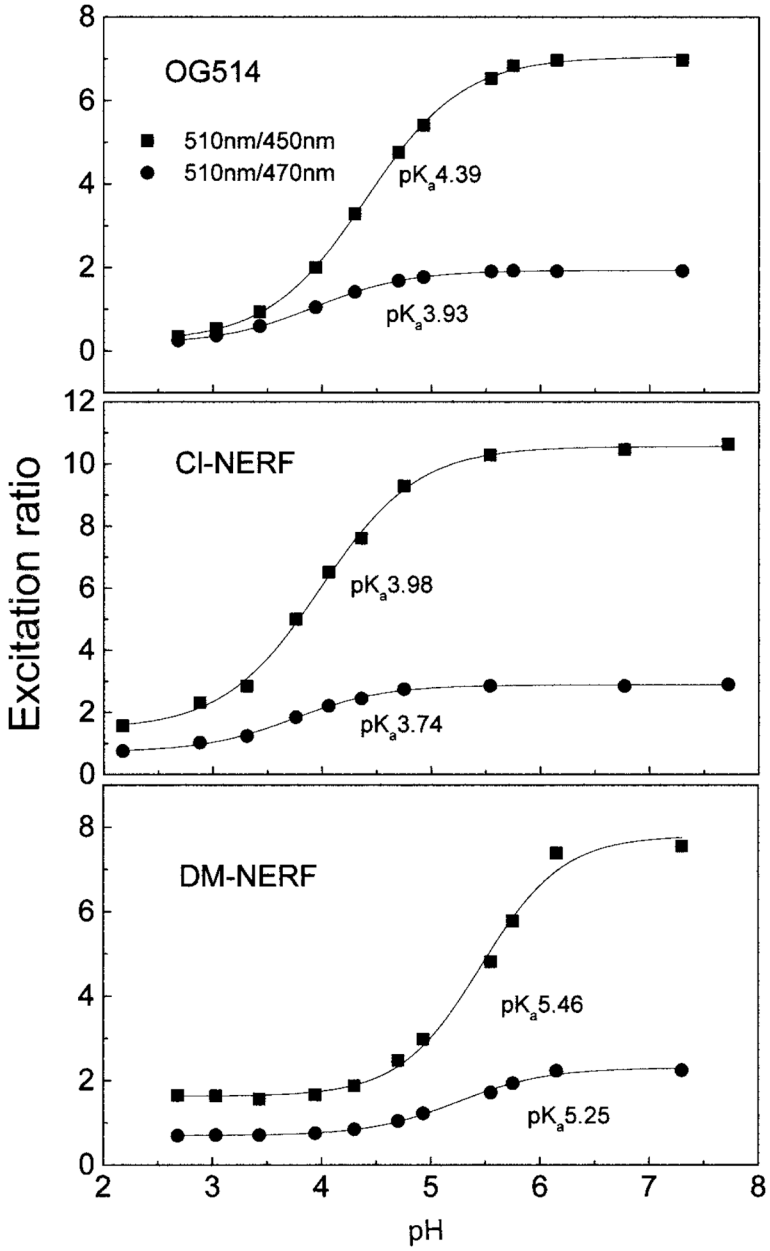

FIG. 3.

The pH dependency of the emission intensity of OG514, Cl-NERF, and DM-NERF based on wavelength-ratiometric measurement. The excitation wavelength pairs used here were 510 nm/450 nm and 510 nm/470 nm, and the emission intensity was monitored at 570 nm.

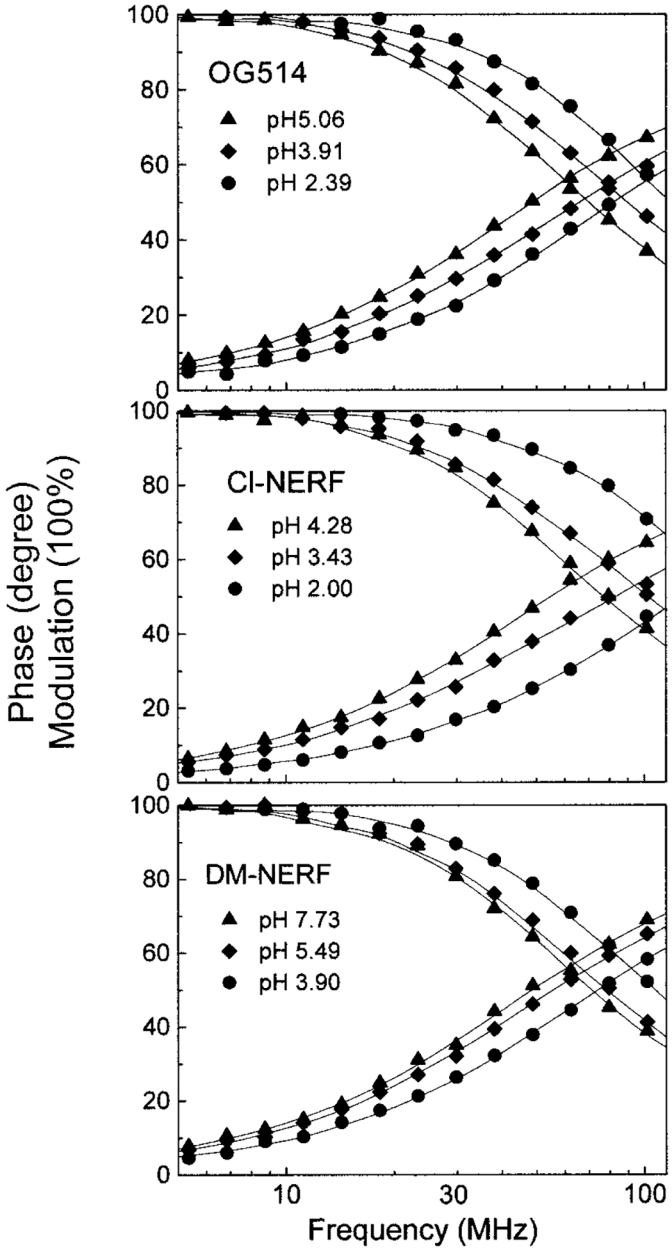

FIG. 4.

Frequency-domain intensity decays of the three probes at different pH values. The excitation wavelength was 488 nm.

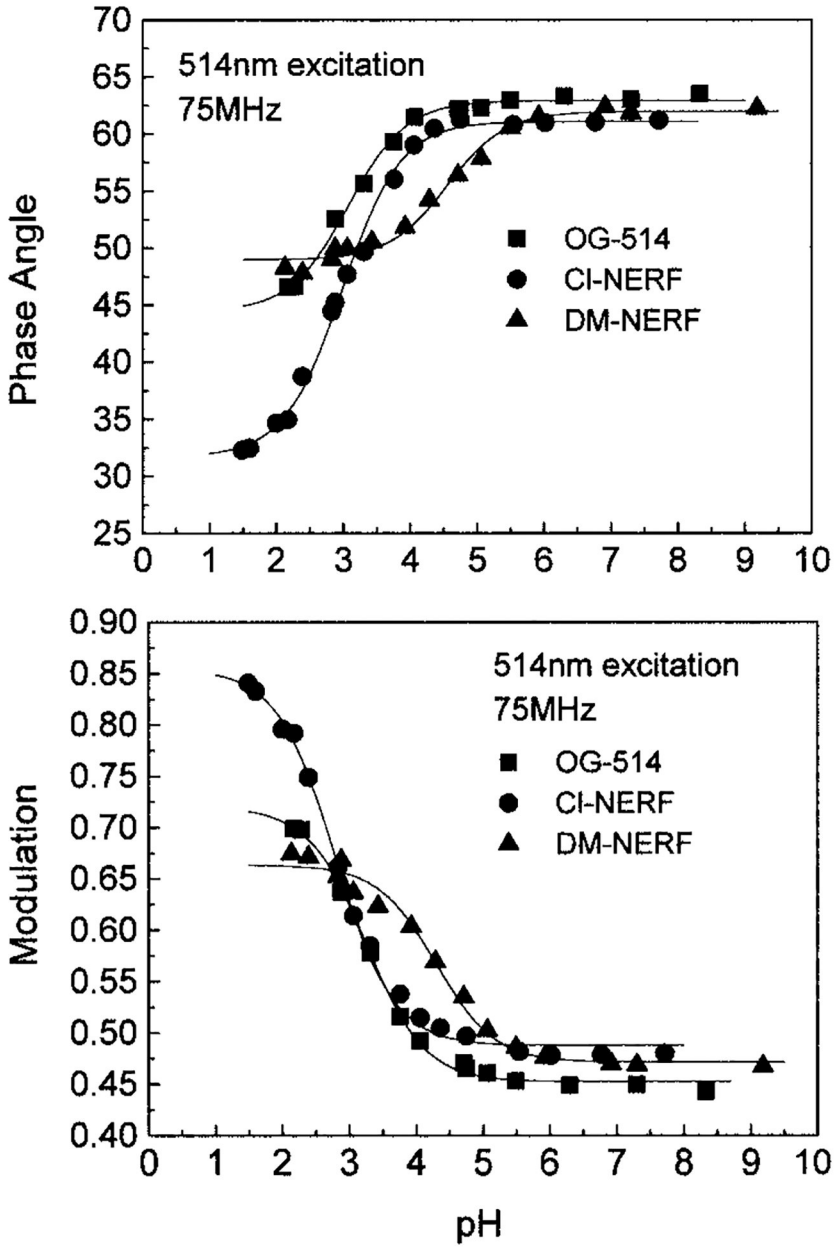

FIG. 5.

The pH dependency of the phase angles and modulations for OG514, Cl-NERF, and DM-NERF.

TABLE 1

Spectral Changes and pK_a Values for the Three pH Probes

	Quantum yield				Phase angle		Modulation	
pH probe	**Protonated**	**Unprotonated**	**pK_a** [a]	**λ_{exc} (nm)**	**pK_a**	**$\Delta\theta$(deg)**	**pK_a**	**Δm**
OG514	0.22	0.65	4.7	488	4.10	15.3	3.77	0.24
				514	3.21	16.3	3.28	0.25
Cl-NERF	0.19	0.78	3.8	488	3.40	27.2	3.08	0.36
				514	3.02	29.1	2.79	0.37
DM-NERF	0.37	0.88	5.4	488	5.35	13.8	5.00	0.19
				514	4.70	13.3	4.30	0.19

[a]The actual pK_a is shown in the first column; apparent phase and modulation pK_a values are also listed.

TABLE 2

Global Intensity Decay Analysis of the pH Probes for a Range of pH Values

pH of the solution	a_1	f_1	$\bar{\tau}$ (ns)[a]
Oregon green 514 carboxylic acid			
3.06	0.916	0.859	2.56
3.43	0.865	0.782	2.70
3.91	0.657	0.518	3.18
4.28	0.431	0.298	3.58
4.71	0.176	0.107	3.93
5.06	0.122	0.072	3.99
5.49	0.000	0.000	4.12
Global decay time: τ_1 = 2.31 ns, τ_2 = 4.12 ns, square root of variance = 3.37.			
Cl-NERF			
2.00	0.936	0.842	1.67
2.39	0.881	0.730	1.93
2.88	0.787	0.576	2.28
3.43	0.550	0.309	2.89
3.91	0.278	0.123	3.31
4.28	0.079	0.030	3.52
Global decay time: τ_1 = 1.31 ns, τ_2 = 3.59 ns, square root of variance = 2.86.			
DM-NERF			
3.43	0.978	0.964	2.47
3.91	0.905	0.854	2.64
4.28	0.861	0.792	2.73
4.71	0.739	0.635	2.97
5.06	0.613	0.494	3.18
5.49	0.349	0.248	3.55
5.93	0.184	0.122	3.74
6.30	0.025	0.016	3.90
7.73	0.019	0.012	3.91
Global decay time: τ_1 = 2.42 ns, τ_2 = 3.93 ns, square root of variance = 3.10.			

[a] $\bar{\tau}$ stands for the mean lifetime and equals to $\Sigma a_i \tau_i^2 / \Sigma a_i \tau_i$.